Postmetallization annealing effect of TiN-gate Ge metal-oxide-semiconductor capacitor with ultrathin SiO_2 / GeO_2 bilayer passivation

Nakashima, Hiroshi
Art, Science and Technology Center for Cooperative Research, Kyushu University

Iwamura, Yoshiaki
Interdisciplinary Graduate School of Engineering Sciences, Kyushu University

Sakamoto, Keita
Interdisciplinary Graduate School of Engineering Sciences, Kyushu University

Wang, Dong
Art, Science and Technology Center for Cooperative Research, Kyushu University

他

https://hdl.handle.net/2324/25535

出版情報：Applied Physics Letters. 98 (25), pp.252102(1)-252102(3), 2011-06. American Institute of Physics
バージョン：

Postmetallization annealing effect of TiN-gate Ge metal-oxide-semiconductor capacitor with ultrathin SiO_2/GeO_2 bilayer passivation

Hiroshi Nakashima,[1,a)] Yoshiaki Iwamura,[2] Keita Sakamoto,[2] Dong Wang,[1] Kana Hirayama,[2] Keisuke Yamamoto,[2] and Haigui Yang[1]

[1]*Art, Science and Technology Center for Cooperative Research, Kyushu University, 6-1 Kasuga-koen, Kasuga, Fukuoka 816-8580, Japan*

[2]*Interdisciplinary Graduate School of Engineering Sciences, Kyushu University, 6-1 Kasuga-koen, Kasuga, Fukuoka 816-8580, Japan*

(Received 27 April 2011; accepted 28 May 2011; published online 20 June 2011)

The postmetallization annealing (PMA) effect was investigated for a TiN-gate Ge metal-oxide-semiconductor capacitor with an ultrathin SiO_2/GeO_2 bilayer passivation. PMA at 450 °C led to the incorporation of nitrogen atoms into the gate stack. Consequently, the flat band voltage shifted from −0.79 to +0.23 V, resulting from a decrease in the dipole at the SiO_2/GeO_2 interface and the accompanying creation of a negative charge. The hysteresis decreased from 98 to 27 mV and the interface state density decreased from 6×10^{11} to 2.5×10^{11} $cm^{-2}\,eV^{-1}$, as results of the nitrogen termination of defects at the SiO_2/GeO_2 interface and/or in the GeO_2 interlayer. © *2011 American Institute of Physics*. [doi:10.1063/1.3601480]

Germanium (Ge) is of great interest as a candidate channel material for future complementary metal-oxide-semiconductor (CMOS) devices owing to its high intrinsic carrier mobility. In realizing Ge-CMOS technology, however, there are many difficulties associated with the different physical and chemical properties of Ge compared with Si. The formation of a good MOS stack is one of the most challenging issues, and many recent studies on this topic have been published.[1]

Recently, we proposed a method for electrical passivation of a Ge surface by an ultrathin SiO_2/GeO_2 bilayer.[2,3] By optimizing this bilayer passivation (BLP) and subsequent gate-insulator deposition, an interface state density (D_{it}) of 4×10^{11} $cm^{-2}\,eV^{-1}$ was achieved near the midgap despite the very thin thickness (1.6 nm) of the GeO_2 layer.[2]

To apply this BLP to a high-permittivity (high-*k*)/Ge gate stack, there are two major topics to be addressed. One is high-*k* film fabrication matched with BLP. Another is the optimization for the metal gate process such as TiN or TaN because such nitrides are important as thermostable electrodes and also for threshold voltage (V_{TH}) control.[4,5] However, the studies on metal gates for fabricating a good Ge-MOS stack are very few.

In this letter, we focused on the TiN metal gate and investigated the effect of postmetallization annealing (PMA) on the electrical properties of a TiN-gate Ge-MOS capacitor. It was found that PMA at 450 °C led to three good effects; significant improvements of hysteresis (HT), flatband voltage (V_{FB}), and D_{it}. We will discuss the role of nitrogen incorporated in the Ge-MOS stack.

A p-type (100) Ge substrate with a resistivity of 0.34 Ω cm was used. First, sacrificial oxidation was performed at 450 °C for 30 min by dry oxidation (GeO_2 thickness: 3 nm), followed by loading a physical vapor deposition (PVD) chamber for BLP. The details of BLP are given elsewhere.[2,3] After complete volatilization of GeO_2 by vacuum annealing, a 1.0-nm-thick SiO_2 interlayer (IL) was deposited on the cleaned Ge surface at 350 °C using rf magnetron sputtering from a SiO_2 target with the addition of O_2. Note that a GeO_2 layer grows during the SiO_2 deposition and its thickness is approximately 1.0 nm.[2,3] Then, a 10-nm-thick SiO_2 film without the addition of O_2 was deposited at room temperature (RT) using the same PVD system, followed by the postdeposition annealing (PDA) at 550 °C for 30 min in N_2. The physical thickness of GeO_2 was found to be increased up to 1.6 nm by the PDA.[2,3]

A 50-nm-thick TiN film was deposited on the SiO_2-gate insulator by rf magnetron sputtering using a TiN target in Ar ambient. During the deposition, the gas pressure was kept at 2.0 Pa. The applied rf power was also kept at 60 W, resulting in a deposition rate of approximately 10 nm/min. The resistivity of the TiN film followed by annealing at 350 °C for 10 min in N_2 was 140 $\mu\Omega$ cm, which was close to the value for stoichiometric TiN film.[6] The PMA of the TiN-deposited sample was performed at temperatures in the range of 350–550 °C for 20 min in N_2. Then, a 100-nm-thick Al film was deposited by thermal evaporation. The gate patterning with an area of 2.25×10^{-4} cm^{-2} was performed by lithography. First, etching for the Al gate electrode was done by H_3PO_4 solution at 40 °C, and second, etching for the TiN electrode was performed by wet etching (1 part NH_4OH, 4 parts H_2O_2) at 50 °C. Note that this wet etching method enables us to perform selective etching of TiN film on SiO_2 and high-*k* dielectrics such as HfO_2 and HfSiON.[7] Finally, contact annealing was carried out at 350 °C for 10 min in N_2 for obtaining electrically good adhesion between Al and TiN films.

Equivalent oxide thicknesses (EOTs) for all fabricated capacitors were approximately 12–13 nm from the capacitance-voltage (C-V_G) measurements. Figure 1 shows the C-V_G curves of the MOS capacitors without PMA and with PMA at 450 °C, for which the measurements were performed at RT and a frequency of 1 MHz. The bias was double-scanned from −2 to +1 V and +1 to −2 V. It is interesting that PMA at 450 °C led to a significant shift in V_{FB} and a drastic decrease in HT. The dependences of V_{FB}

[a)]Electronic mail: nakasima@astec.kyushu-u.ac.jp.

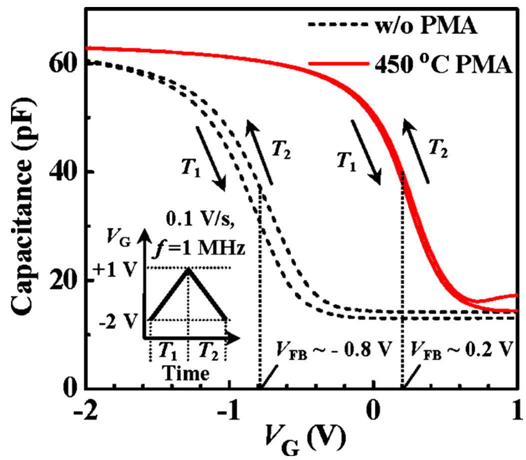

FIG. 1. (Color online) C-V_G characteristics for TiN-gate Ge-MOS capacitors without PMA and with PMA at 450 °C.

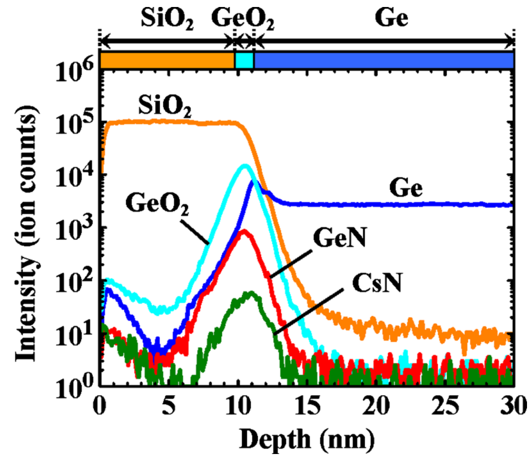

FIG. 3. (Color online) TOF-SIMS results. Cs and Bi^{3++} ions were used for etching and analysis, respectively. TiN film was removed by wet etching.

and HT on PMA temperature (T_{PMA}) are shown in Figs. 2(a) and 2(b), respectively. The HT drastically decreased with an increase in T_{PMA} and achieved a minimum value of 27 mV at 450 °C. The V_{FB} monotonically increased with an increase in T_{PMA} and showed +0.23 V at 450 °C. It is likely that nitrogen atoms in TiN film diffused into SiO_2 and affected the electrical properties of the Ge-MOS gate stack.

To clarify the presence of nitrogen in the gate stack, time-of-flight-secondary ion mass spectroscopy (TOF-SIMS) measurements (Cs and Bi^{3++} ions were used for the etching and analysis, respectively) were performed for a sample with PMA at 450 °C, where the TiN film on the sample was completely removed by wet etching. Figure 3 shows the TOF-SIMS results. The GeN and CsN signals were clearly observed, and the locations completely coincided with that of GeO_2 signal, implying that nitrogen exists in the GeO_2 IL between SiO_2 and Ge.

To clarify the origin of the V_{FB} shift, we investigated the effective work function ($\Phi_{m,eff}$) and the fixed charge density (Q_f) by V_{FB} versus EOT plots for Ge and Si substrates.[8] For Si substrates, Al/TiN/SiO_2/Si structures were prepared using the same processes as those for Ge. Since the EOT of the SiO_2-gate insulator is much thicker than that of the GeO_2 IL, the relation between V_{FB} and EOT is given by $V_{FB}=(\Phi_{m,eff}-\Phi_{Ge/Si})-Q_f\times \mathrm{EOT}/\varepsilon_{ox}$, where $\Phi_{Ge/Si}$ is the work function of the Ge or Si substrate, and ε_{ox} is the dielectric constant of SiO_2. Thus, Q_f can be calculated from the slope of the V_{FB}-EOT plot, and $\Phi_{m,eff}$ can be estimated from the V_{FB}-intercept value.

The V_{FB}-EOT plots for Ge and Si substrates are shown in Fig. 4. The obtained $\Phi_{m,eff}$ and Q_f are summarized in Table I. It can be seen from the $\Phi_{m,eff}$ results for Si that $\Phi_{m,eff}$ changed from 4.55 to 4.68 eV after PMA at 450 °C. It has been reported that the $\Phi_{m,eff}$ of a TiN film on SiO_2 prepared from reactive magnetron sputter deposition using Ti target changes from 4.2 to 4.9 eV with an increase in the nitrogen content.[6] Furthermore, the $\Phi_{m,eff}$ of stoichiometric TiN deposited by atomic layer deposition was reported to be around 5.0 eV.[4] Thus, the small increase in $\Phi_{m,eff}$ found in this letter is likely to be attributed to the near-stoichiometry of TiN film.

On the other hand, we can find interesting phenomena from $\Phi_{m,eff}$ results for Ge and Si. The difference (ΔV_{dip}) between $\Phi_{m,eff}$ values for Ge and Si corresponds to V_{FB} shift by electric dipole formation at SiO_2/GeO_2 interface because the TiN/SiO_2 interface should be the same for both cases of Ge and Si. The values of ΔV_{dip} are listed in Table I. Recently, Kita and Toriumi[9] have proposed an areal density difference model of oxygen atoms at high-k/SiO_2 interfaces to explain

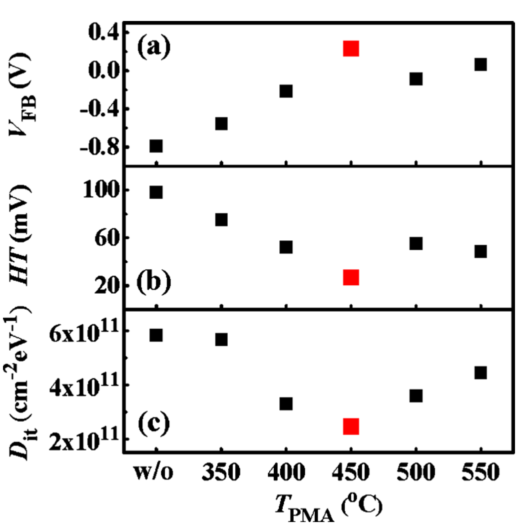

FIG. 2. (Color online) Dependences of (a) V_{FB}, (b) HT, and (c) D_{it} on PMA temperature (T_{PMA}).

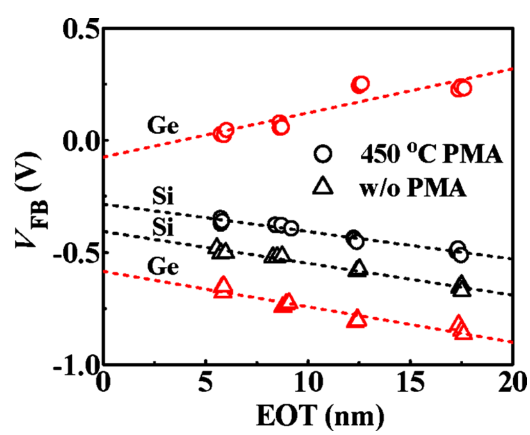

FIG. 4. (Color online) V_{FB}-EOT plots for Ge and Si substrates. The heat treatments were no-PMA and 450 °C-PMA.

TABLE I. $\Phi_{m,eff}$ and Q_f obtained from V_{FB}-EOT plots.

PMA	$\Phi_{m,eff}$ (eV) Si	Ge	ΔV_{dip} (eV)	Q_f (10^{11} cm^{-2}) Si	Ge
w/o	4.55	3.92	−0.63	(+)3.1	(+)3.4
450 °C	4.68	4.42	−0.26	(+)2.6	(−)4.2

the physical origin of the dipole formed at high-k/SiO_2 interface. If we apply this model to the present results, oxygen atoms are transferred from GeO_2 to SiO_2 at the interface. This movement leads to negatively charged interstitial oxygen (O_I^-) in SiO_2 and positively charged oxygen vacancy (O_V^+) in GeO_2. As a result, the dipole layer causes a decrease in $\Phi_{m,eff}$ of TiN. In other words, the V_{FB} shifts by interface dipole formation at SiO_2/GeO_2 were −0.63 and −0.26 V for MOS capacitors without PMA and with PMA at 450 °C, respectively. This means that the PMA at 450 °C led to a decrease in the amount of the dipole. The modulation of TiN's $\Phi_{m,eff}$ in the range of 3.9–4.4 eV (indicated in Table I) is very attractive from the view point of the V_{TH} control of Ge-MOS transistor.

Another important factor in understanding the role of nitrogen in SiO_2/GeO_2 gate stack is Q_f. The Q_f in the Si-MOS capacitor with the 450 °C-PMA was $+3\times10^{11}$ cm^{-2} and almost the same as that without PMA, as listed in Table I. This suggests that nitrogen atoms cannot terminate the dangling bonds in SiO_2 or there is no dangling bond in SiO_2. By contrast, the Q_f in the Ge-MOS capacitor changed from $+3.4\times10^{11}$ to -4.2×10^{11} cm^{-2} after the 450 °C-PMA, which is likely to be associated with a decrease in dipole. Since the strength of the dipole depends on the amount of the dipole, the nitrogen incorporated in the gate stack may induce the reaction of $(O_I^-/O_V^+)^0 \rightarrow (O^-/O_V^+-N^-)^-$ at the SiO_2/GeO_2 interface, resulting in negative fixed charges.

Figure 5 shows D_{it} distributions for Ge-MOS capacitors with and without PMA. The D_{it} was measured by deep-level transient spectroscopy (DLTS),[2] where an injection pulse for the hole capture was set at an accumulated bias (V_{AP}) of −2 V, and a quiescent reverse bias (V_R) corresponding to a band bending of ϕ_B (ϕ_B: the energy between Fermi-level and intrinsic Fermi-level) was set for hole emission, as shown in Fig. 5. Although the D_{it} values near the valence band edge were almost the same for all capacitors, the D_{it} near the midgap decreased with an increase in T_{PMA} up to 450 °C. The D_{it} values near the midgap are plotted in Fig. 2(c). The PMA at 450 °C led to the lowest D_{it} of 2.5 $\times10^{11}$ cm^{-2} eV^{-1}, indicating that 450 °C-PMA is also effective for decreasing D_{it}. The decreasing tendency of D_{it} with T_{PMA} is very similar to that of HT. Since HT is associated with defect-related slow traps at the SiO_2/GeO_2 interface and/or in the GeO_2 IL,[10] a decrease in HT should be caused by nitrogen terminations of the slow traps responsible for the trapping phenomenon. Similarly, it is likely that the D_{it} values near the midgap reflect not only fast traps due to GeO_2/Ge interfacial defects but also slow traps at the SiO_2/GeO_2 interface and/or in a GeO_2 IL. If so, when the V_{AP} is small, the electric field for the hole injection into a GeO_2 IL becomes weak, and the D_{it} should be decreased.

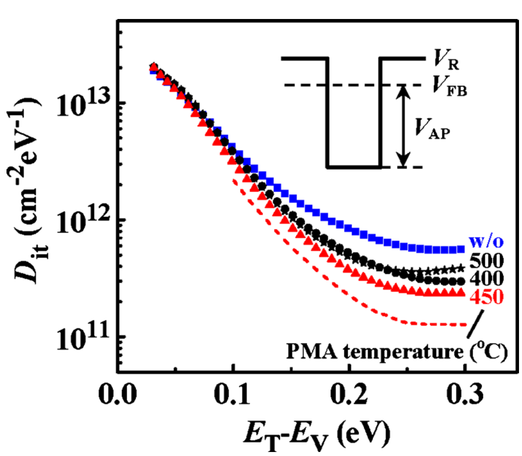

FIG. 5. (Color online) D_{it} distributions for TiN-gate Ge-MOS capacitors with various PMA treatments. The DLTS measurements were performed at an emission rate of 545 s^{-1}, a pulse width of 20 μs, and a V_{AP} of −2 V. The D_{it} distribution shown by the broken line was measured at a V_{AP} of −0.5 V.

To clarify the contribution of the slow traps, we performed DLTS measurements for a MOS capacitor with 450 °C-PMA with a V_{AP} of −0.5 V. The obtained result is shown by a broken line in Fig. 5. It is clear that D_{it} decreased down to 1.2×10^{11} cm^{-2} eV^{-1} near the midgap, which agrees well with the reported D_{it} value of GeO_2/Ge.[11] Therefore, we suppose that the good PMA effect on D_{it} for a capacitor with very thin GeO_2 IL results from the dangling bond termination by nitrogen at the SiO_2/GeO_2 interface and/or in GeO_2 IL. The detailed dependence of D_{it} distribution on V_{AP} will be reported as another paper.

In summary, we clarified the PMA effect for a TiN-gate Ge-MOS capacitor with BLP. PMA at 450 °C led to a positive V_{FB} shift, small HT, and low D_{it}. The V_{FB} shift was mainly due to a decrease in the amount of dipole at the SiO_2/GeO_2 interface and the accompanying creation of negative charge centers. The decreases in HT and D_{it} were attributable to the termination of defects at the SiO_2/GeO_2 interface and/or in GeO_2 IL.

This work was supported in part by a Grant-in-Aid for Scientific Research (Grant No. 21246054) from the MEXT.

[1] C. Claeys and E. Simoen, *Germanium-Based Technologies*, 1st ed. (Elsevier, Oxford, 2007), p. 295.
[2] K. Hirayama, K. Yoshino, R. Ueno, Y. Iwamura, H. Yang, D. Wang, and H. Nakashima, Solid-State Electron. **60**, 122 (2011).
[3] K. Hirayama, R. Ueno, Y. Iwamura, K. Yoshino, D. Wang, H. Yang, and H. Nakashima, Jpn. J. Appl. Phys. **50**, 04DA10 (2011).
[4] J. Westlinder, T. Schram, L. Pantisano, E. Cartier, A. Keber, G. S. Lujan, and J. Olsson, IEEE Electron Device Lett. **24**, 550 (2003).
[5] Y. Sugimoto, K. Yamamoto, and H. Nakashima, Jpn. J. Appl. Phys., Part 2 **46**, L211 (2007).
[6] J. Westlinder, G. Sjoblom, and J. Olsson, Microelectron. Eng. **75**, 389 (2004).
[7] Y. Sugimoto, M. Kajiwara, K. Yamamoto, Y. Suehiro, D. Wang, and H. Nakashima, Appl. Phys. Lett. **91**, 112105 (2007).
[8] D. K. Schroder, *Semiconductor Material and Device Characterization* 3rd ed. (Wiley, New Jersey, 2006), p. 335.
[9] K. Kita and A. Toriumi, Appl. Phys. Lett. **94**, 132902 (2009).
[10] D. Kuzum, T. Krishnamohan, A. Nainani, Y. Sun, P. A. Pianetta, H. S.-P. Wong, and K. Saraswat, Tech. Dig. - Int. Electron Devices Meet. **2009**, 453.
[11] H. Matsubara, T. Sasada, M. Takenaka, and S. Takagi, Appl. Phys. Lett. **93**, 032104 (2008).